Electronic Supplementary Material (ESI) for ChemComm.

Supporting Information

A Chemo-mechanical Switch for Controllable Water Transportation Based on Thermally Responsive Block Copolymer

Jianmin Yang, Mitsuaki Hida, Sifeng Mao, Hulie Zeng, Hizuru Nakajima, and Katsumi Uchiyama*

Department of Applied Chemistry, Graduate School of Urban Environmental Sciences, Tokyo Metropolitan University, Minamiohsawa, Hachioji, Tokyo 192-0397, Japan

Corresponding Author

E-mail: uchiyama-katsumi@tmu.ac.jp; Tel: +81-42-6772835, Fax: +81-42-6772821

1. Materials and chemicals

Capillary plates（1.0 mm thick） with a pore size of 6.0 μm were purchased from Hamamatsu Photonics (type J5022-09, Hamamatsu, Japan). Quartz glass plates（1.0 mm thick），18 mm × 18 mm in size were purchased from Matsunami Glass Ind., Ltd (Tokyo, Japan). N-isopropylacrylamide (NIPAAm) was obtained from Kohjin Co. Ltd. (Tokyo, Japan), and recrystallized before use. Hexafluoroisopropyl acrylate (HFIPA), 3-aminopropyltrimethoxysilane (APTMS, 97%), 2-bromoisobutyryl bromide (BIBB, 97%), copper(I) bromide (CuBr), N,N-dimethylformamide (DMF, 99.8%), sodium chloride (99.7%), ethanol (99%), methanol (99.99%), sulfuric acid (98%), N, N, N′, N″, N″-pentamethyl diethylenetriamine (PMDTA, 98%), toluene (super-dehydrated), dichloromethane (super dehydrated) and pyridine (dehydrated) were all purchased from Wako Pure Chemical Co. (Tokyo, Japan). Deionized water obtained from a Direct-Q™5 Nihon Millipore ultrapure water system (Tokyo, Japan).

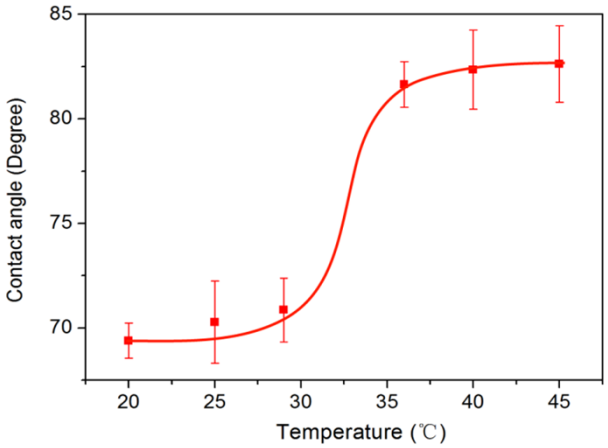

Figure S1. Temperature dependences of water CA for the PNIPAAm brush on a flat glass plate.

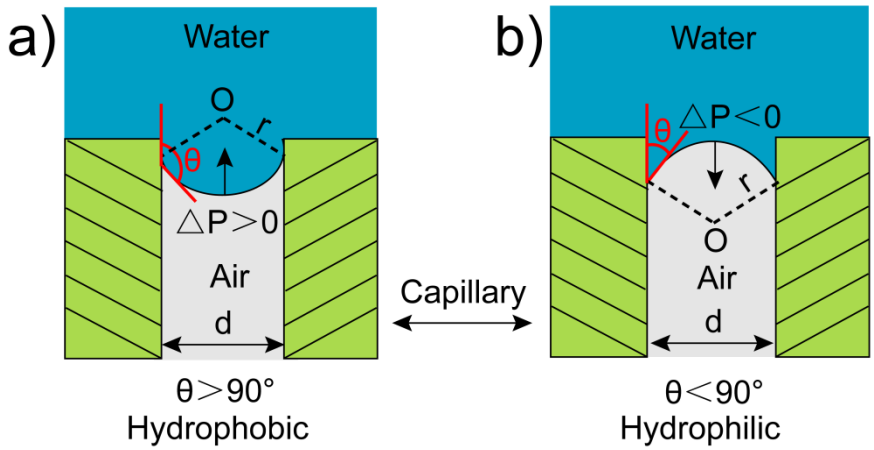

Figure S2. Schematic diagram of the liquid wetting model of the capillary plate. (a) For the hydrophobic state, a water contact angle $\theta > 90°$. Unless external pressure is applied, the water cannot permeate through the plate because of the static pressure $\Delta P > 0$ (negative capillary effect). (b) For the hydrophilic state, $\theta < 90°$, the capillary plate cannot withstand any pressure because the static pressure $\Delta P < 0$ (capillary effect); and the water can permeate the plate spontaneously. The position O denotes the center of the spherical cap that describes the meniscus; r is the radius of the meniscus; d is the pore size of the capillary plate.

In Figure S2, the differential pressure, ΔP, across the meniscus, which can be described as the eq 1.[1-3]

$$\Delta P = 2\gamma_{LV}/r \qquad (1)$$

where γ_{LV} is the surface tension of the liquid–vapor interface, r is the radius of meniscus.

Herein, $r = d/2\cos(180°-\theta)$, so eq 1 can be reorganized as eq 2.

$$\Delta P = -4\gamma_{LV}(\cos\theta)/d \qquad (2)$$

or eq 3

$$\Delta P = -l\gamma_{LV}(\cos\theta)/A \qquad (3)$$

where d is the pore size of the capillary plate, l is the circumference of the pore, A is the cross-sectional area of the pore, and θ is the advancing contact angle of liquid on the surface.

2. Synthesis of the P(NIPAAm-co-HFIPA)-grafted surfaces

P(NIPAAm-co-HFIPA) was synthesized using the process of surface-initiated atom transfer radical polymerization (ATRP) and the entire polymerization process was depicted in Figure S3.

2.1 Activation

The substrate (capillary plate or glass plate) was successively sonicated for 5 min in acetone and deionized water, respectively. The substrate was then sonicated with 0.1 M NaOH solution for 10 min to generate –OH groups on the surface. Afterward, the substrate was washed with deionized water by sonicated, and then dried under vacuum.

2.2 Amine functionalization

Subsequently, the surface of substrate was aminated by treatment with a 10% v/v APTMS solution in anhydrous toluene. After refluxing for 6 h at 130°C, excess APTMS was removed by washing with toluene and dichloromethane. The substrate was then dried under a vacuum.

2.3 Amidation

The substrate was immersed in anhydrous dichloromethane with additional pyridine (2% v/v). After cooling the above solution to 0°C for 1 h in the ice bath, 2-bromoisobutyryl bromide, a polymerization initiator, was added to the solvent (0.5% v/v). The ice bath was removed after 5 min and the reaction allowed to warm to room temperature, and the reaction was allowed to proceed for 12 h with stirring to generate the initiator grafted surface. Subsequently, the substrate was washed with acetone and toluene, and then dried under a vacuum.

2.4 Polymerization

Regarding the process of PNIPAAm, the substrate was reacted with a degassed PNIPAAm solution (containing 1.0 g NIPAAm crystallization, 5 mL methanol, 5 mL DMF, 0.23 mL PMDETA, and 0.032 g CuBr) at 60°C for 2 h. In the case of P(NIPAAm-co-HFIPA), the substrate was reacted with a degassed

PNIPAM solution at 60°C for 1 h, 0.4 mL of HFIPA was then added to the solution and the reaction was allowed to proceed for another 1 h at 60°C. Finally, the polymer-grafted surfaces were washed 3 times each with deionized water and acetone and dried under a vacuum.

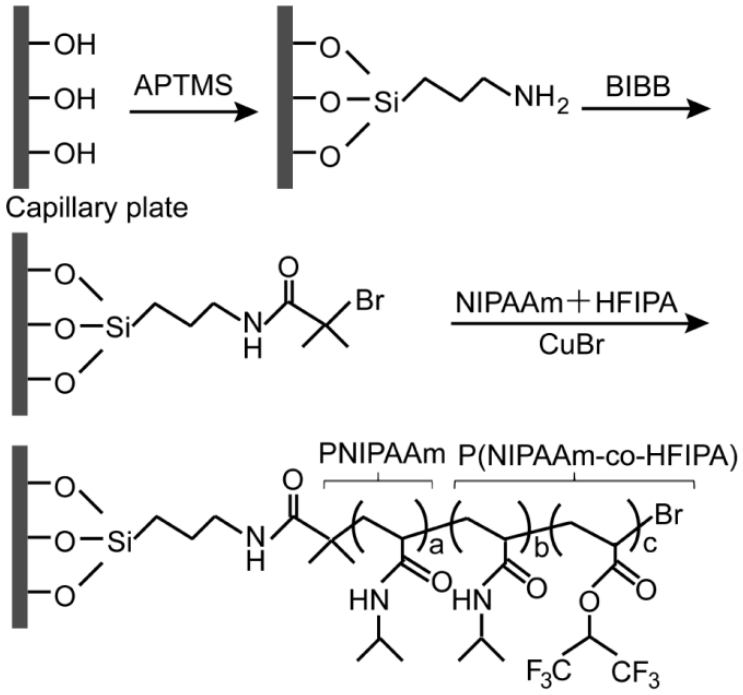

Figure S3. Synthesis of the P(NIPAAm-co-HFIPA) copolymer brush by surface-initiated atom transfer radical polymerization (ATRP) on capillary plate surface.

3. EDX characterization

A scanning electron microscope combined with X-ray energy dispersive spectrometer (SEM-EDX, S-3400N, Hitachi, Japan) was used to examine the morphology and chemical composition of the surface of the capillary plate before and after modification. EDX characterization for each polymerization process is shown in Figure S4. The results confirm that the copolymer film was successfully grafted on the capillary plate.

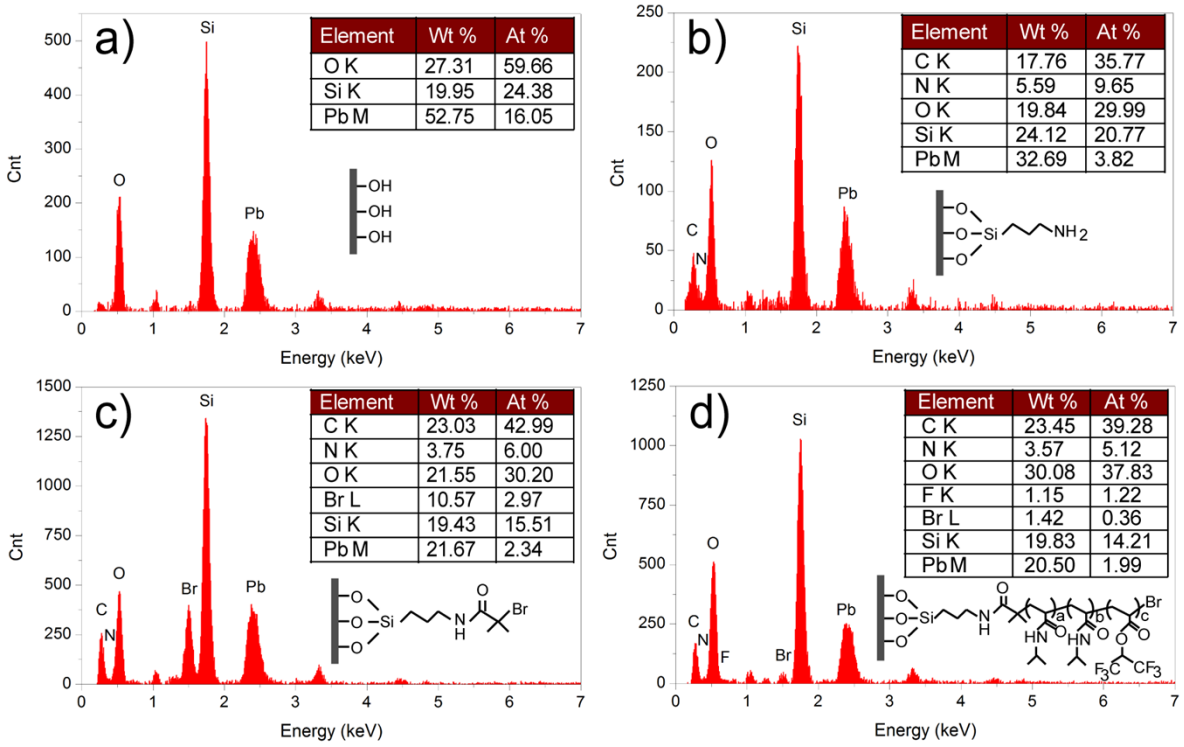

Figure S4. EDX characterization for each polymerization process. (a) Bare capillary plate. (b) Amine functionalization. (c) Amidation. (d) Polymerization. The relative contents of each element for each polymerization process are shown in the figure.

4. Wenzel and Cassie–Baxter equation

On a smooth and chemically homogeneous surface, as illustrated in Figure S5 (left), the contact angle (CA), θ_S, is given by Young's equation, eq 4

$$\cos\theta_S = (\gamma_{sv} - \gamma_{sl})/\gamma_{lv} \quad (4)$$

where the γ_{lv}, γ_{sl}, and γ_{sv} are the liquid–vapor, solid–liquid and solid–vapor interfacial tensions, respectively. When the surface is roughness, the theories that are commonly used to correlate the surface roughness with the apparent CA of a liquid droplet on a solid substrate are the Wenzel and Cassie–Baxter equations.

In the Wenzel case,[4] as shown in Figure S5 (middle), the liquid completely fills the grooves of the rough surface where they contact, described by eq 5

$$\cos\theta_W = r\cos\theta_S \quad (5)$$

where θ_W is the apparent CA in the Wenzel mode and r is the surface roughness factor.

In the Cassie–Baxter theory,[5] as illustrated in Figure S5 (right), vapor pockets are assumed to be trapped underneath the liquid. Defining the apparent CA in the Cassie mode as θ_{CB}, θ_{CB} can be described by eq 6

$$\cos\theta_{CB} = \varphi_s(\cos\theta_S + 1) - 1 \quad (6)$$

where φ_s is defined as the solid fraction upon which the drop rests.

In our work, the surface of polymer coating capillary plate was hydrophilic when the temperature set at 20 °C. The Wenzel mode contact was formed after the water dripped on the surface. From eq 5, it can be found that if the CA of a liquid on a smooth surface is less than 90°, the apparent angle on a rough surface will be smaller. Thus, the CA decreased from 74.8° on a flat glass plate to 56.1° (capillary plate). Whereas, at 40 °C, the surface of polymer coating capillary plate was hydrophobic which prevented the surface wetting by any aqueous solution. Therefore, the Cassie–Baxter's contact mode was easily

generated at the initially moment when the rough and hydrophobic surface encounter water droplet. From eq 6 it can be found that the surface roughness will increase the apparent CA. So, the water CA increased from 94.3° on a flat glass plate to 118.7° (capillary plate).

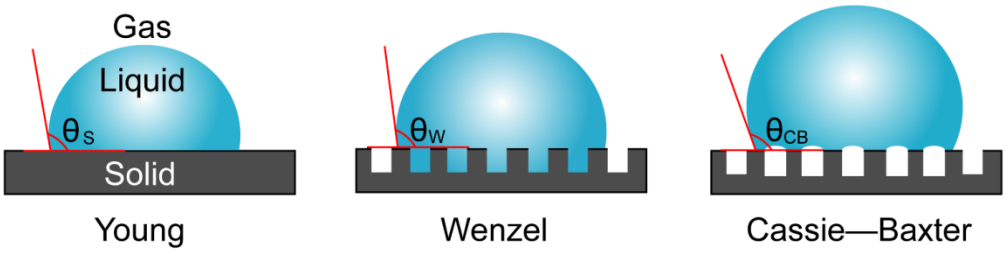

Figure S5. Effect of surface structure on the wetting behavior of solid substrates. (Left) A liquid drop on a flat substrate (Young's mode). (Middle) Wetted contact between the liquid and the rough substrate (Wenzel's mode). (Right) Non-wetted contact between the liquid and the rough substrate (Cassie–Baxter's mode). Reference from Jiang *et al.*[6] and Guo *et al.* [7] work.

5. Contact angle measurement

The water contact angle (CA) on the different substrates was measured by a self-assembled measurement system under conditions of saturated humidity, as shown in Figure S6. A thermoelectric cooler (OCE-F15P-D12, OHM Electric Co., Ltd., Japan) was used to control the temperature. After the system temperature became stable, 5.0 μL of deionized water was dropped carefully onto the surface of the substrates by micro pipette. Images of the water droplet were then obtained with a Dino-Lite digital microscope (AM7013MT, AnMo Electronics Corporation, Taiwan). The water CA was measured by a half angle formula based on the image of the water droplet. Measurements were made at several different positions on each substrate, and the average of these values was determined.

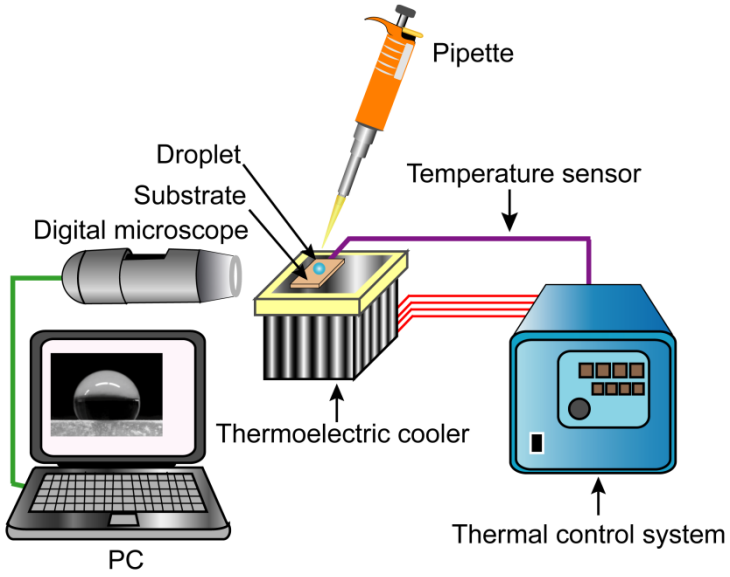

Figure S6. Schematic illustration of the setup for water CA measurement.

6. Process of aqueous solution transportation

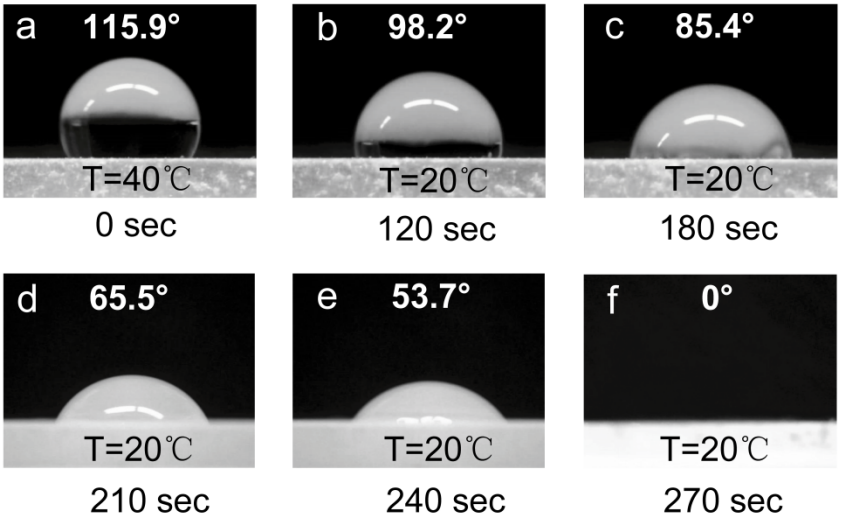

Figure S7. Water droplet transportation process for a single cycle from 40°C to 20°C. (a) Images of the water droplet on the surface of capillary plate were obtained when the system temperature was set as 40°C. Cooling the system temperature to 20°C and the cooling procedure required nearly 120 sec (b). (c-f) Images of the droplet were recorded at 30-sec intervals with the temperature maintained at 20°C. The whole process for a single cycle was complete within 4.5 min.

7. X-ray photoelectron spectroscopy (XPS) characterization

XPS analyses were performed on an ESCA-3400 spectrometer (Shimadzu Co., Kyoto, Japan) equipped with a Mg Kα source (1253.6 eV) operating at 10 kV and 10 mA. The N/Si ratios at different reaction times were listed in **Table S1**.

Table S1. XPS elemental analysis of the surface modified APTMS at different reaction times.

Time (h)	0.5	1.0	2.0	4.0	8.0
N/Si ratio	1.33	1.43	1.94	2.21	2.22

Supporting References

1 J. P. Youngblood and T. J. McCarthy, *Macromol*ecules, 1999, **32**, 6800.

2 B. Liu and F. F. Lange, *J. Colloid Interface Sci.,* 2006, **298**, 899.

3 D. Tian, X. Zhang, X. Wang, J. Zhai and L. Jiang, *Phys. Chem. Chem. Phys.,* 2011, **13**, 14606.

4 R. N. Wenzel, *Ind. Eng. Chem.*, 1936, **28**, 988.

5 A. B. D. Cassie, and S. Baxter, *Trans. Faraday Soc.*, 1944, **40**, 546.

6 X. Feng and L. Jiang, *Adv. Mater.*, 2006, **18**, 3063.

7 B. Wang, Y. Zhang, L. Shi, J. Li and Z. Guo, *J. Mater. Chem.*, 2012, **22**, 20112.